

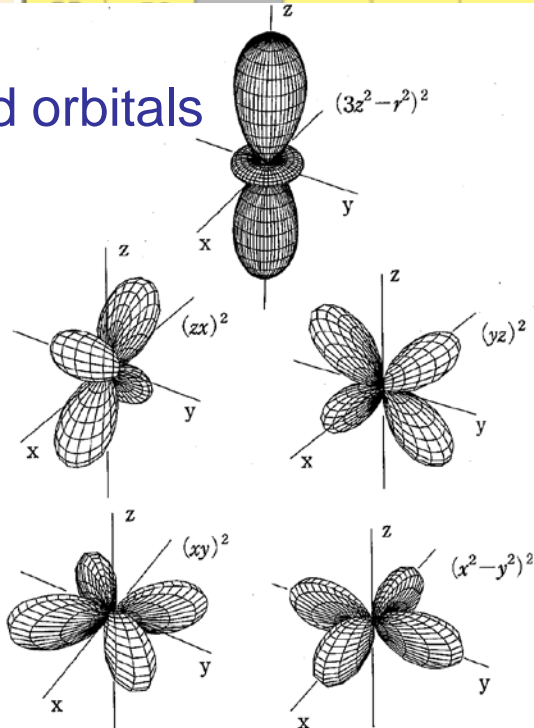
Behind the Scenes of High Temperature Superconductivity: Cuprates and Iron Pnictides

Yukawa Institute for Theoretical Physics

Takami Tohyama
Eiji Kaneshita
Takao Morinari

3d transition-metal compounds

3d orbitals



Localized and itinerant natures compete.



Complicated interactions among the internal degrees of freedom of electrons:
charge, spin, orbital

Cuprate superconductors

The periodic table shows the elements from Hydrogen (H) to Radium (Ra). A blue box highlights the transition metals from Scandium (Sc) to Zinc (Zn), which includes Sc, Ti, V, Cr, Mn, Fe, Co, Ni, Cu, and Zn. A red box highlights Oxygen (O), located in the second column of the second row.

1																			18
1	H	2																	He
3	4																		10
Li	Be																		Ne
11	12																		
Na	Mg	3	4	5	6	7	8	9	10	11	12								
19	20	21	22	23	24	25	26	27	28	29	30	31	32	33	34	35	36		
K	Ca	Sc	Ti	V	Cr	Mn	Fe	Co	Ni	Cu	Zn	Ga	Ge	As	Se	Br	Kr		
37	38	39	40	41	42	43	44	45	46	47	48	49	50	51	52	53	54		
Rb	Sr	Y	Zr	Nb	Mo	Tc	Ru	Rh	Pd	Ag	Cd	In	Sn	Sb	Te	I	Xe		
55	56	57~	72	73	74	75	76	77	78	79	80	81	82	83	84	85	86		
Cs	Ba	71	Hf	Ta	W	Re	Os	Ir	Pt	Au	Hg	Tl	Pb	Bi	Po	At	Rn		
87	88	89~	104	105	106	107	108	109	110	111	112								
Fr	Ra	103	Rf	Db	Sg	Bh	Hs	Mt											

1986 High-temperature superconductivity

$T_c \sim 160\text{K}$ under pressure

Oxides, two-dimensionality \rightarrow superconductivity

Iron-pnictide superconductors

The image shows a standard periodic table with several regions highlighted. A blue rectangular box surrounds the transition metals from Scandium (Sc) to Iron (Fe), and the next two columns (Cobalt (Co) and Nickel (Ni)). A red rectangular box highlights the element Iron (Fe). The noble gases (He, Ne, Ar, Kr, Xe, Rn) are also highlighted in yellow.

1																				18
1	H																			He
3		4																		
Li		Be																		
11		12																		
Na	Mg		3	4	5	6	7	8	9	10	11	12								
19	20		21	22	23	24	25	26	27	28	29	30								
K	Ca		Sc	Ti	V	Cr	Mn	Fe	Co	Ni	Cu	Zn								
37	38		39	40	41	42	43	44	45	46	47	48								
Rb	Sr		Y	Zr	Nb	Mo	Tc	Ru	Rh	Pd	Ag	Cd								
55	56		57~	72	73	74	75	76	77	78	79	80								
Cs	Ba		71	Hf	Ta	W	Re	Os	Ir	Pt	Au	Hg								
87	88		89~	104	105	106	107	108	109	110	111	112								
Fr	Ra		103	Rf	Db	Sg	Bh	Hs	Mt											

2008 Hosono's Group at TIT

$$T_c \sim 55K$$

Fe: typical magnetic metal → superconductivity

OUTLINE

Motivation

Similarity and difference between cuprate and iron-pnictide superconductors

Cuprates

- Ionic material
- doped Mott insulator

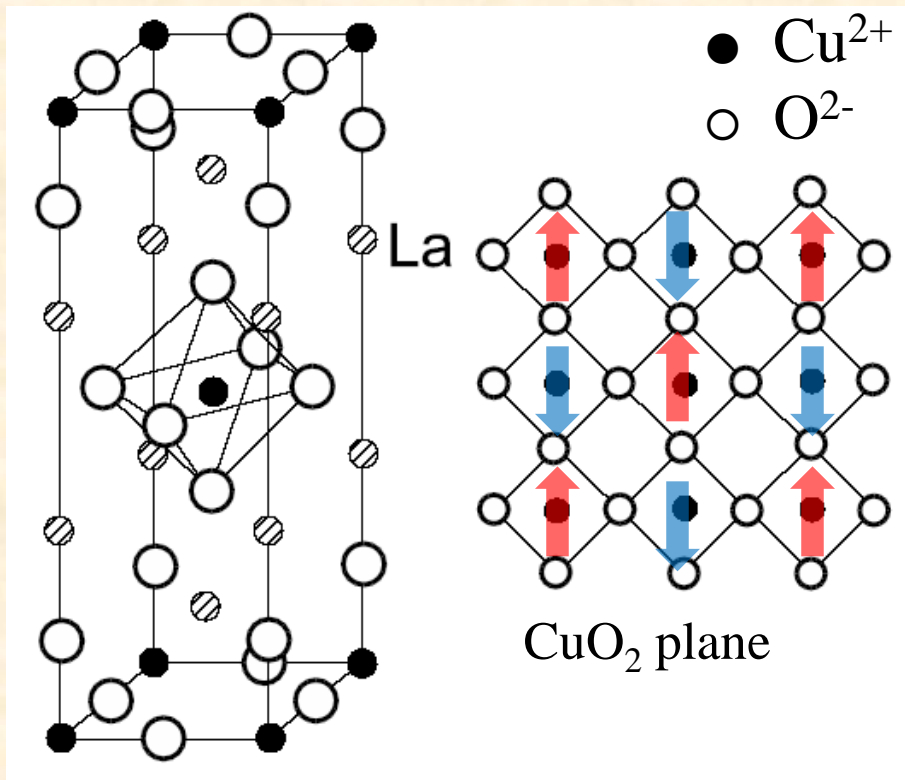
Iron pnictides

- band material
- spin-density wave (SDW)

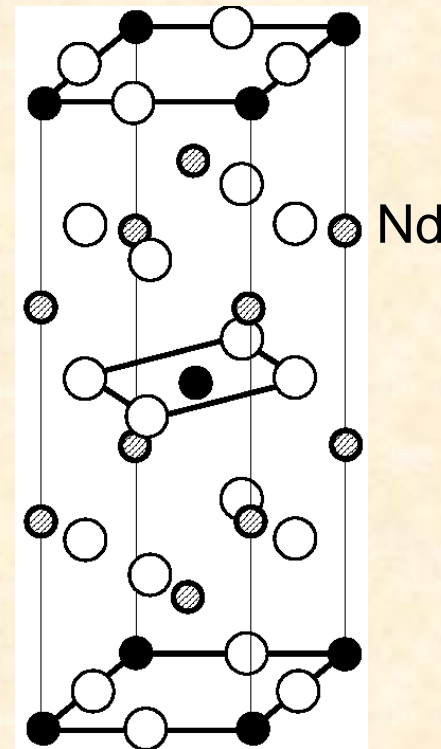
Summary and perspectives

Crystal structure of high T_c cuprates

La_2CuO_4 (hole-doping)



Nd_2CuO_4 (electron-doping)



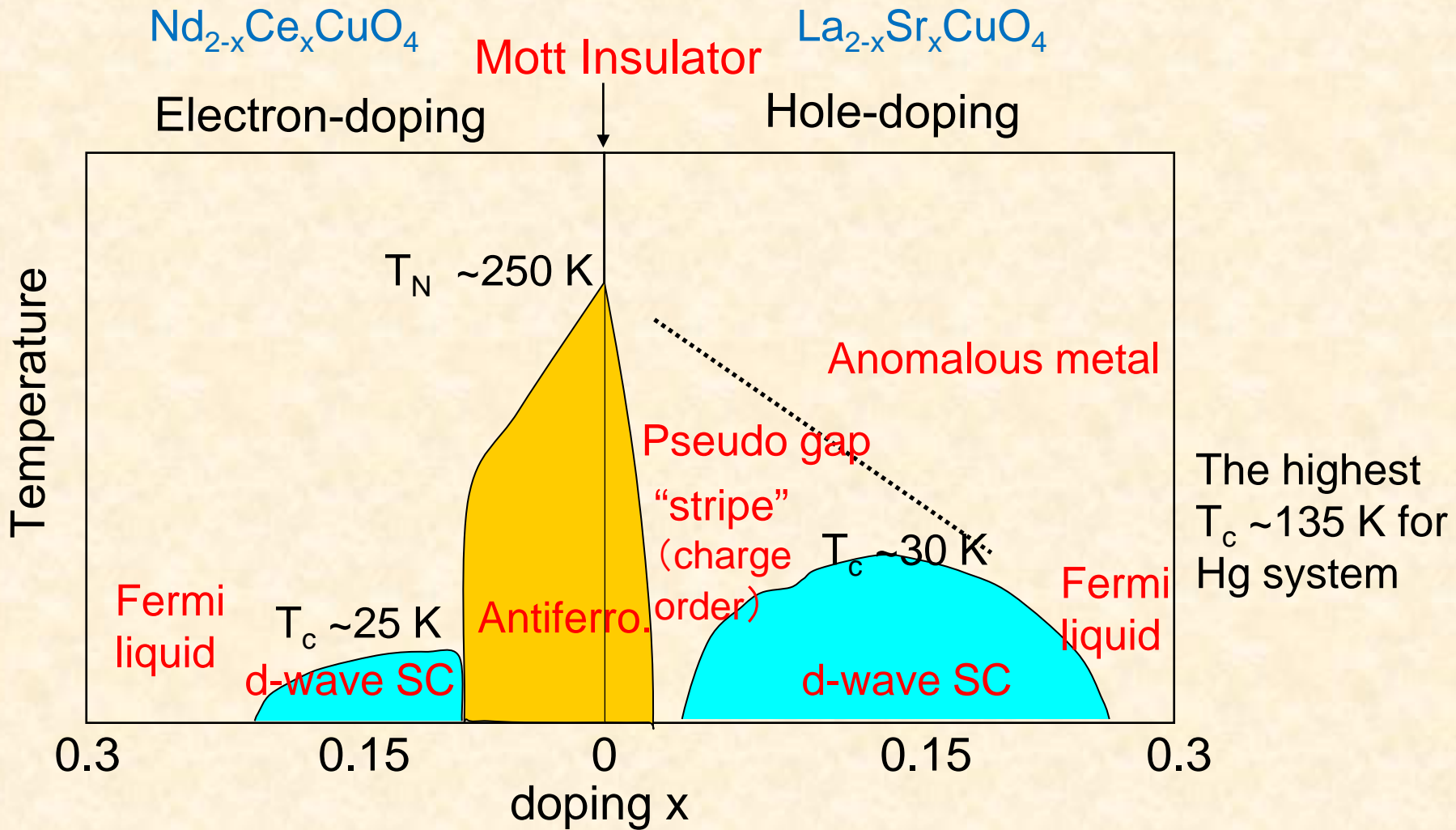
$\text{Cu}^{2+} \ 3d^9 \ S=1/2$ hole on each x^2-y^2 orbital

Strong local Coulomb interaction → Mott insulator

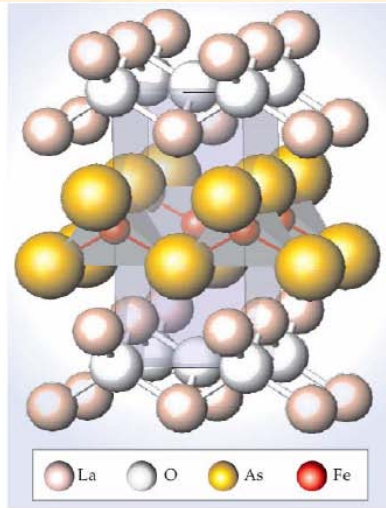
localized spin → antiferromagnetic exchange interaction

$J \sim 1400\text{K}$

Phase diagrams

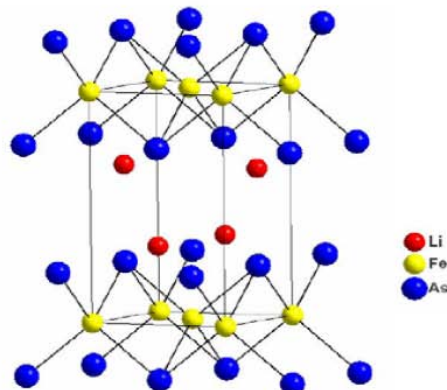


Crystal structure of high T_c iron pnictides



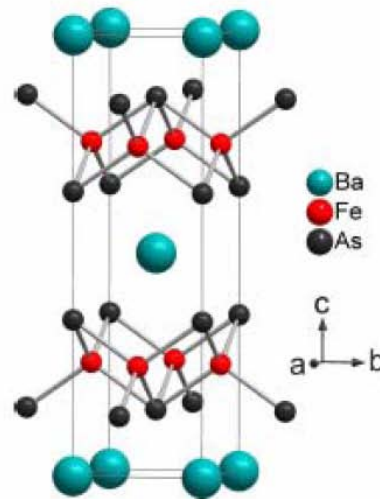
LnFeAsO (1111)

$T_c \sim 55$ K



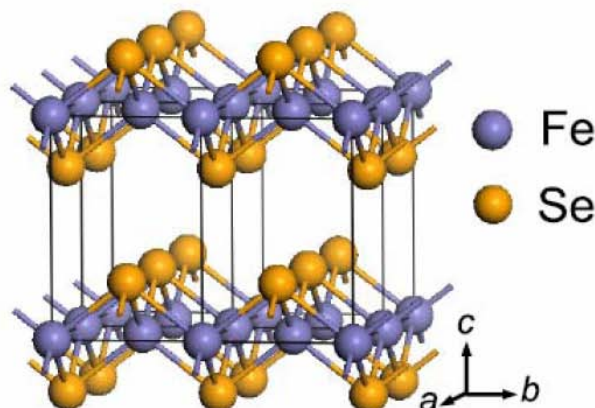
LixFeAs (111)

$T_c \sim 33$ K



BaFe₂As₂ (122)

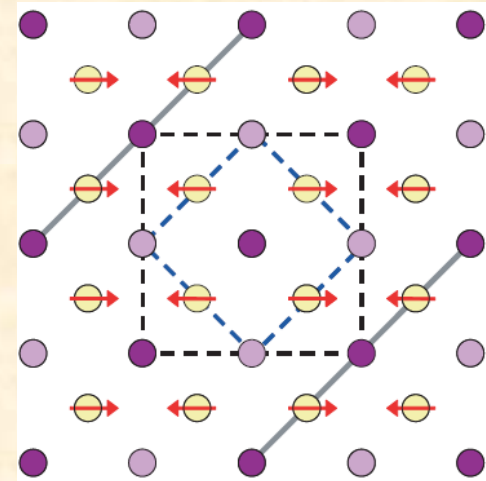
$T_c \sim 37$ K



$T_c \sim 37$ K (under press.)

Layered structures

Fe-As layer
Quasi-2D system



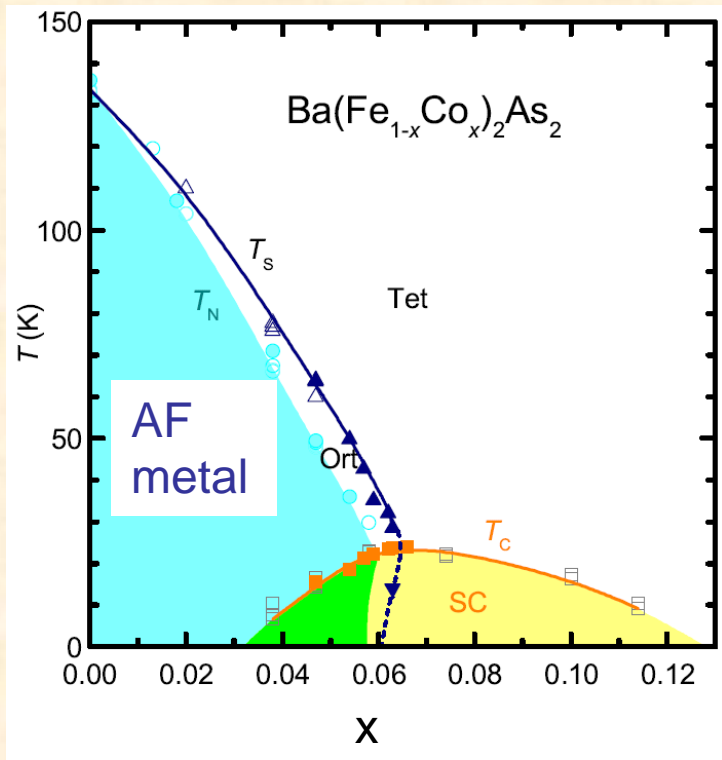
● Fe/Co
● As (Top)
● As (Bottom)

$Q=(\pi, 0)$
“Stripe”order

Phase diagram of high- T_c iron pnictides



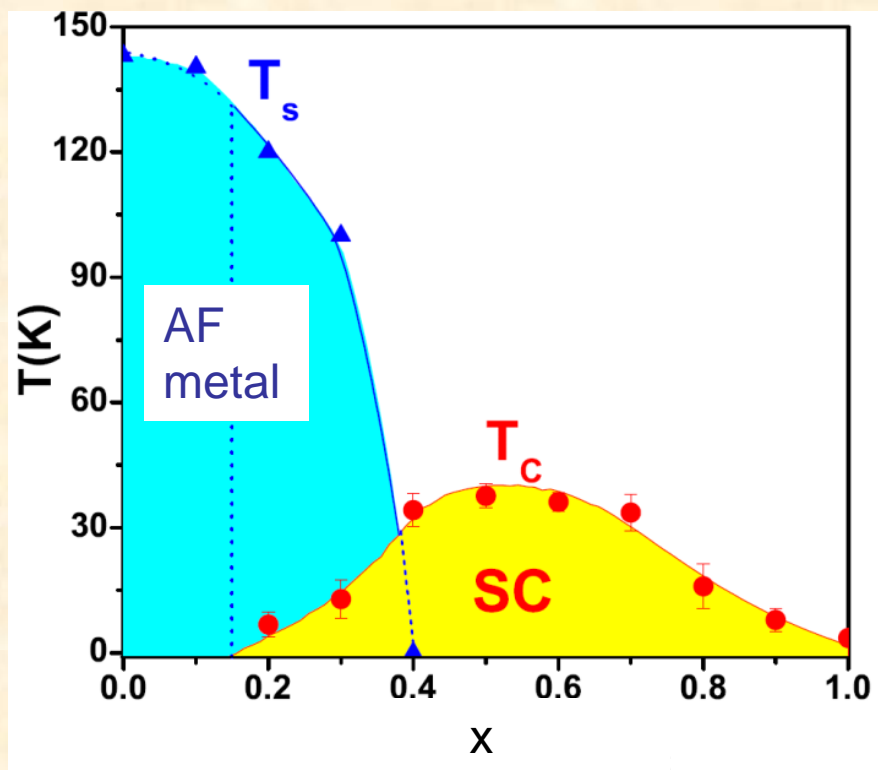
Electron “doping”



S. Nandi *et al.*, PRL **104**, 057006 (2010)



Hole “doping”



H. Chen *et al.*, Europhys. Lett. **85**, 17006 (2009)

Cuprates and iron pnictides

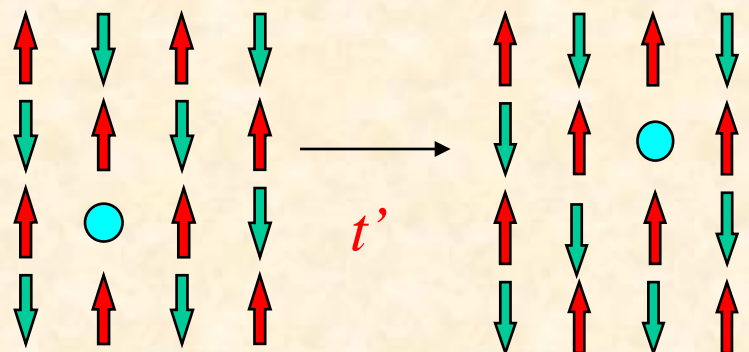
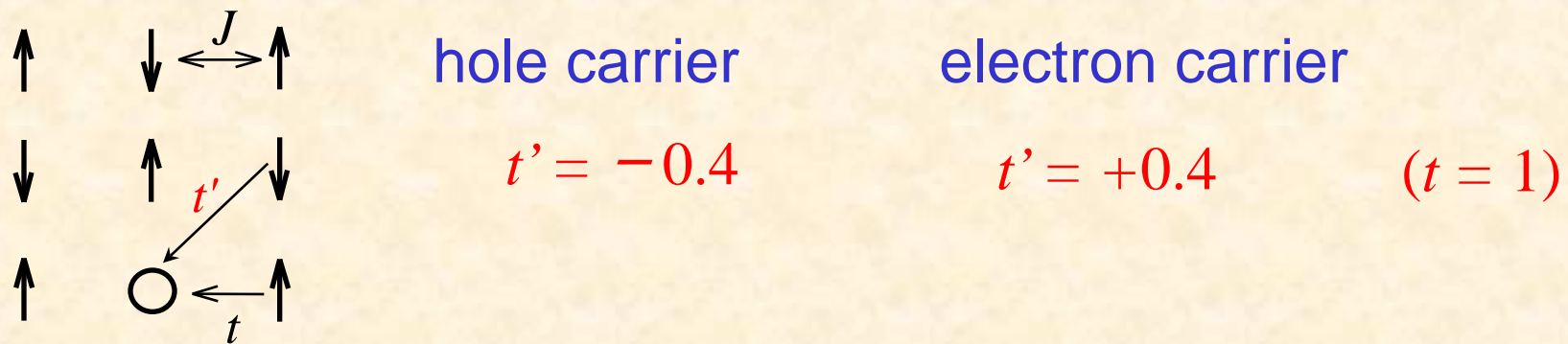
Similarity Superconductivity next to magnetism

Difference	cuprates	iron pnictides
electronic structure	crystal-field, $3d^9$ single band (x^2-y^2)	hybridization, $3d^6$ multi band (five orbitals)
magnetism	Antiferro. insulator	Antiferro. metal
super-conductivity	carrier doping	carrier doping pressure
super-conductivity	$d_{x^2-y^2}$ symmetry	sign-reversed or preserved s anisotropic s, d ??
	approaches from ionic picture and doped Mott insulator	approaches from band picture and spin-density wave

Origin of the electron-hole asymmetry in cuprates

- low-energy effective model: *t-J model*
 - Introduction of the second nearest-neighbour hopping t'

$$H_{tJ} = -t \sum_{\langle i,j \rangle_1, \sigma} \tilde{c}_{i,\sigma}^+ \tilde{c}_{j,\sigma} + J \sum_{i\delta} \mathbf{S}_i \cdot \mathbf{S}_{i+\delta} - t' \sum_{\langle i,j \rangle_2, \sigma} \tilde{c}_{i,\sigma}^+ \tilde{c}_{j,\sigma}$$



No change of spin configuration by t'

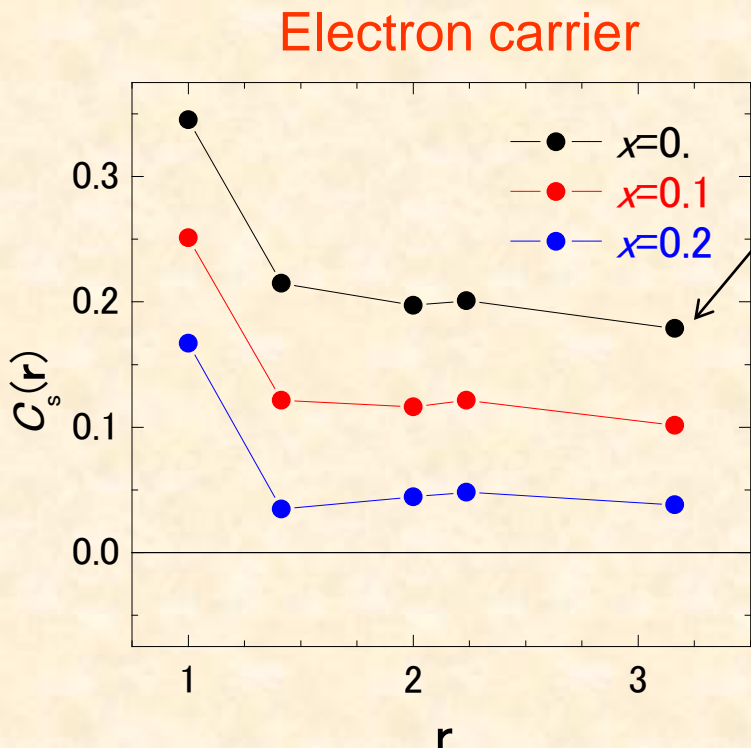
The magnitude of the self-energy of this configuration is dependent of the sign of t'

Asymmetry of spin-spin correlation function

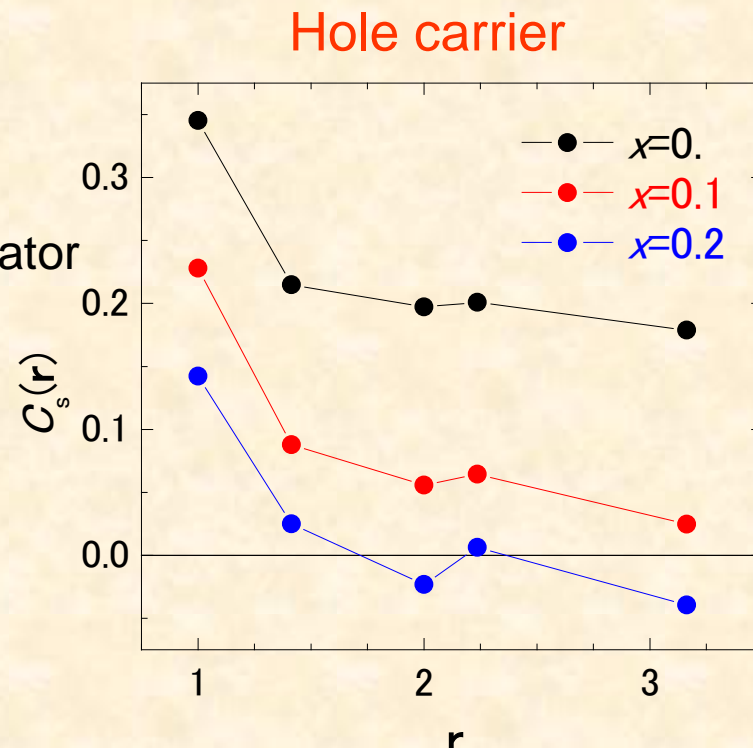


Exact results for a
20-site t-t'-J model

x : carrier density

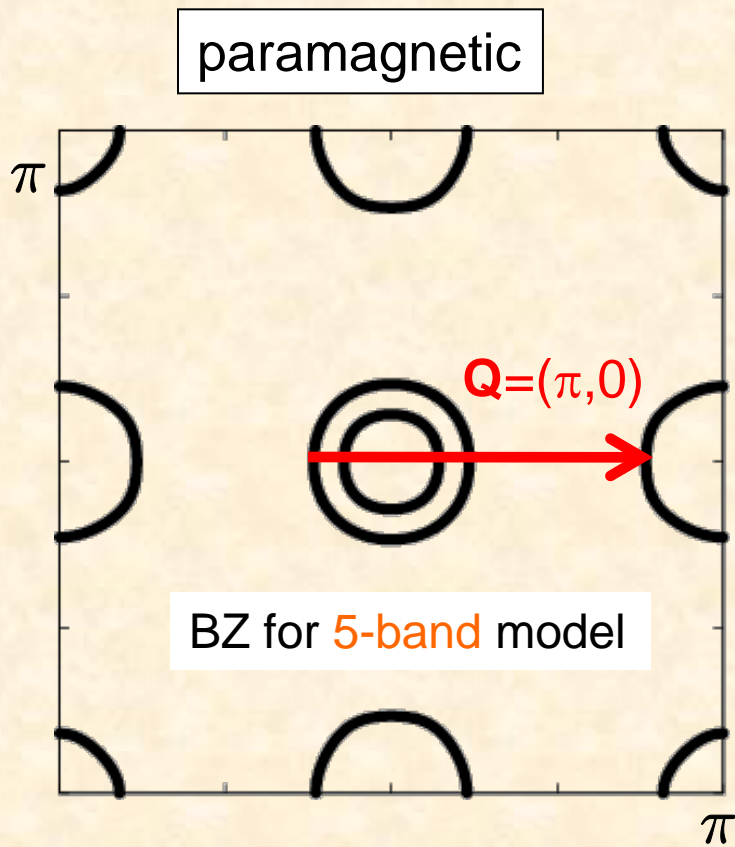


Mott
insulator



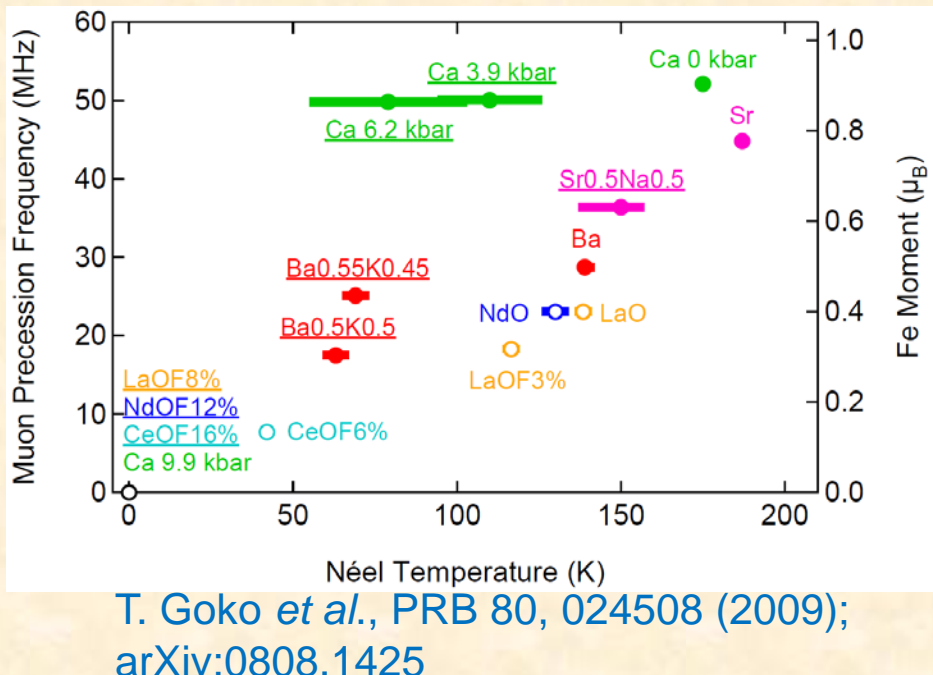
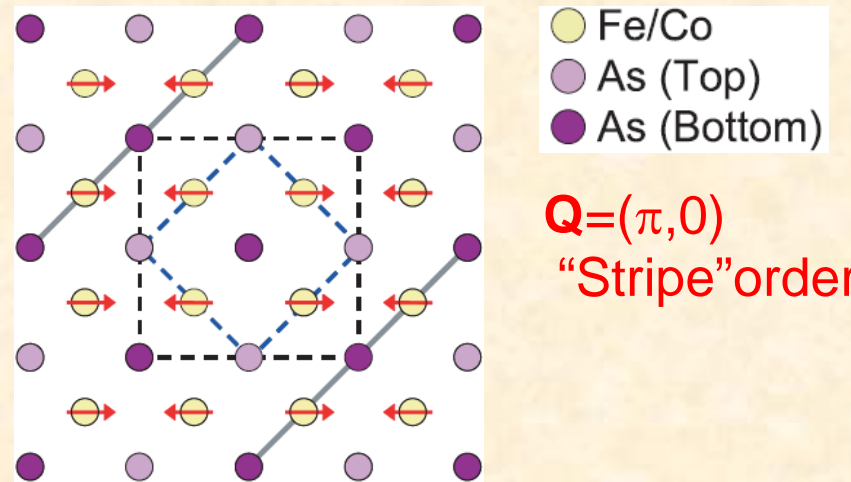
Antiferromagnetic correlation survives for the electron carrier.

Antiferromagnetic phase of iron pnictides



5-band tight-binding model
[K. Kuroki *et al.*, PRL 101, 087004 (2008)]

spin-density wave (SDW) ?

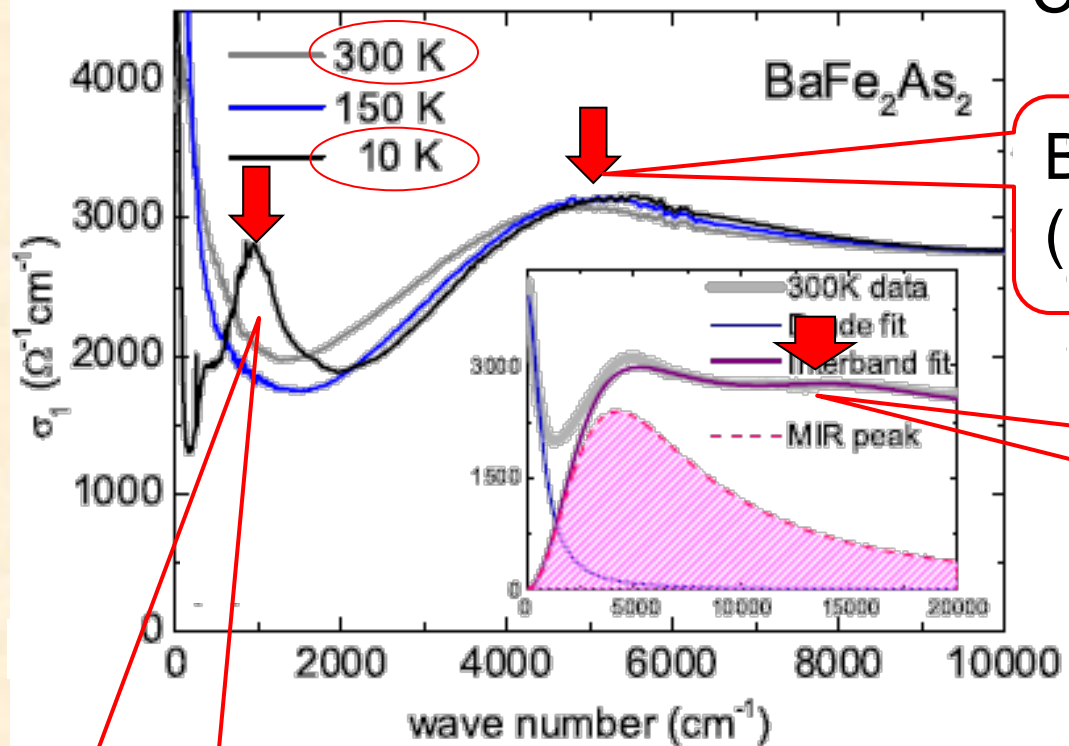


T. Goko *et al.*, PRB 80, 024508 (2009);
arXiv:0808.1425

Characteristics of optical conductivity

grey
black

Compare PM and AF data



AF gap (~0.1eV)

Broad excitation structure (~0.5eV) slightly shifted

Unchanged in high energies

W. Z. Hu et al., PRL 10, 257005 (2008)

Mean-field calculation of the stripe AF state

Five-band model for the Fe square lattice

$$H = H_0 + H_I$$

$$H_0 = \sum_{\mathbf{k}, \mu, \nu, \sigma} \left[\sum_{\Delta} t(\Delta_x, \Delta_y; \mu, \nu) e^{i\mathbf{k}\cdot\Delta} + \epsilon_{\mu} \delta_{\mu, \nu} \right] c_{\mathbf{k}\mu\sigma}^{\dagger} c_{\mathbf{k}\nu\sigma}$$

K. Kuroki et al., Phys. Rev. Lett. **101**, 087004 (2008)

$$\begin{aligned} H_I = & U \sum_{i, \mu} n_{i\mu\uparrow} n_{i\mu\downarrow} + \frac{2U - 5J}{4} \sum_{i, \mu \neq \nu, \sigma, \sigma'} n_{i\mu\sigma} n_{i\nu\sigma'} \\ & + J \sum_{i, \mu \neq \nu} (c_{i\mu\uparrow}^{\dagger} c_{i\nu\uparrow} c_{i\mu\downarrow}^{\dagger} c_{i\nu\downarrow} - \mathbf{S}_{i\mu} \cdot \mathbf{S}_{i\nu}) \end{aligned}$$

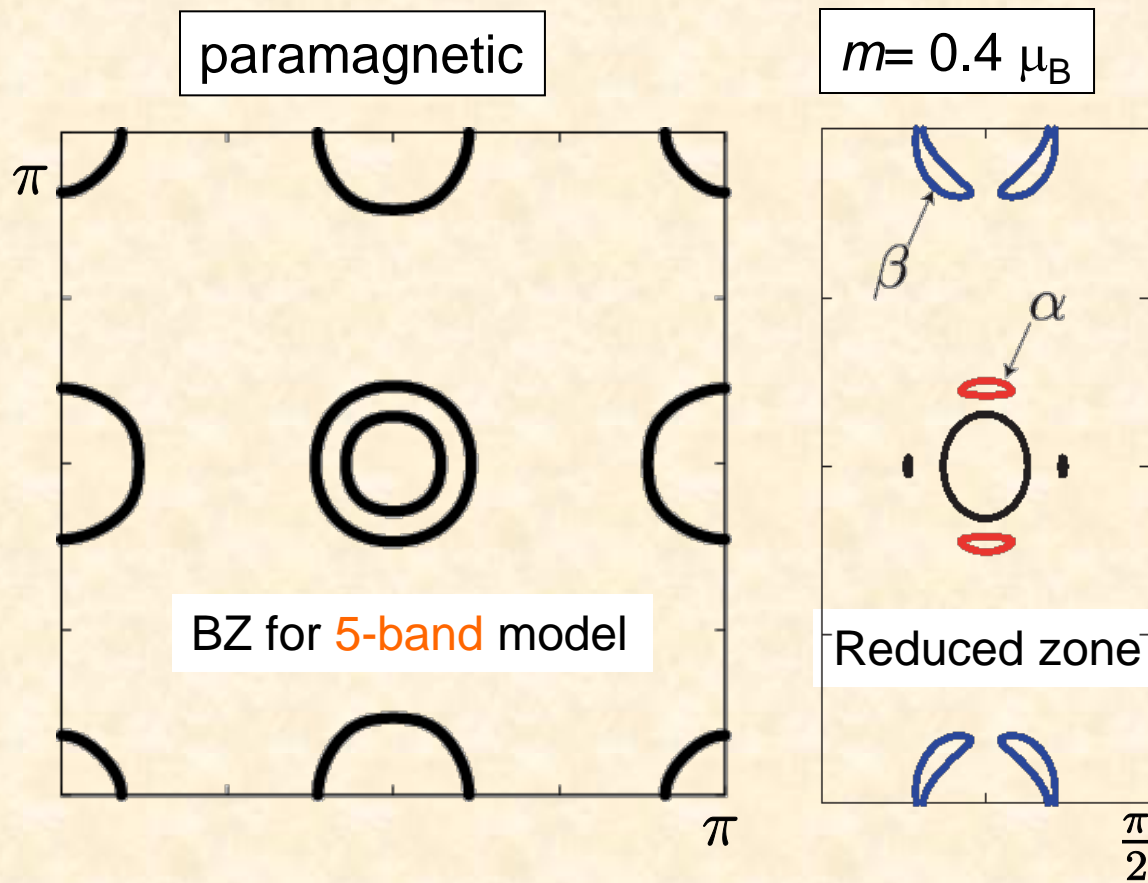
Striped AF order

Order parameter

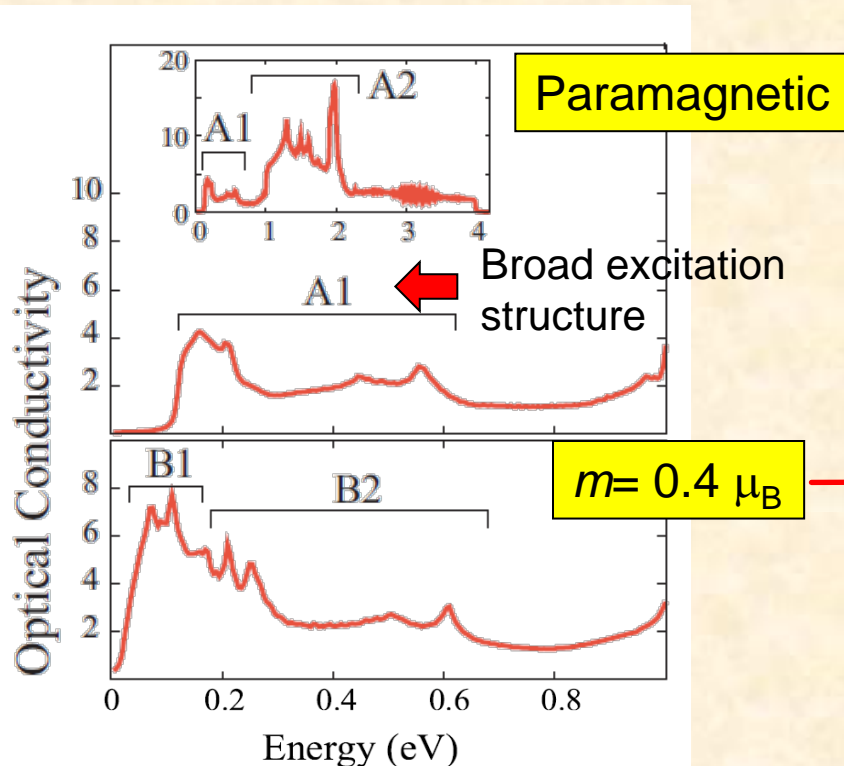
$$\langle n_{\mathbf{Q}\mu\nu\sigma} \rangle = \frac{1}{N} \sum_{\mathbf{k}} \langle c_{\mathbf{k}+\mathbf{Q}\mu\sigma}^{\dagger} c_{\mathbf{k}\nu\sigma} \rangle$$

$m = 0.4 \mu_B$

Fermi surfaces



Calculated optical conductivity (Interband transitions)



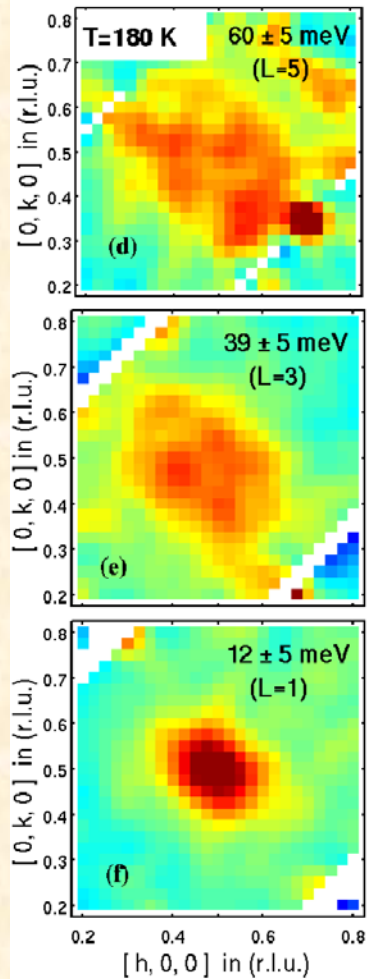
- #1: SDW gap state (~0.1eV)
(B1)
- #2: Small shift of broad structure
(A1 → B2)
- #3: No change
in high energy > 0.5eV
(Similar DOS)

The AF state exhibits optical conductivity consistent with experiments.

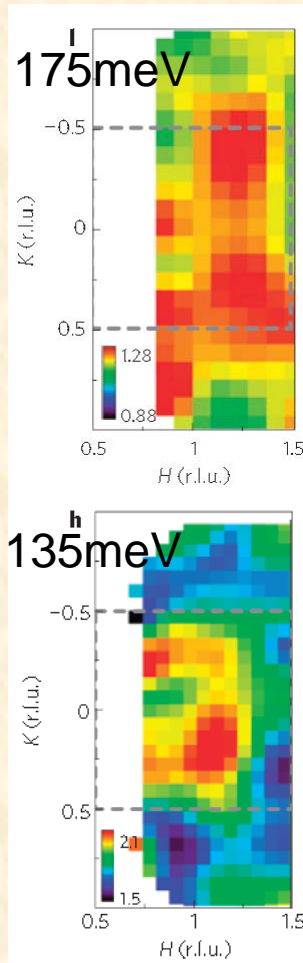
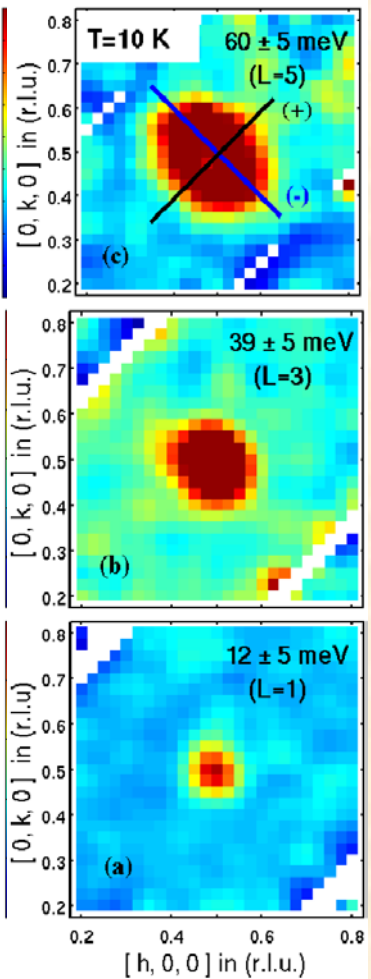
E. Kaneshita, T. Morinari, T.T., PRL 103, 224519 (2009)

Spin excitation of CaFe_2As_2 Experiment

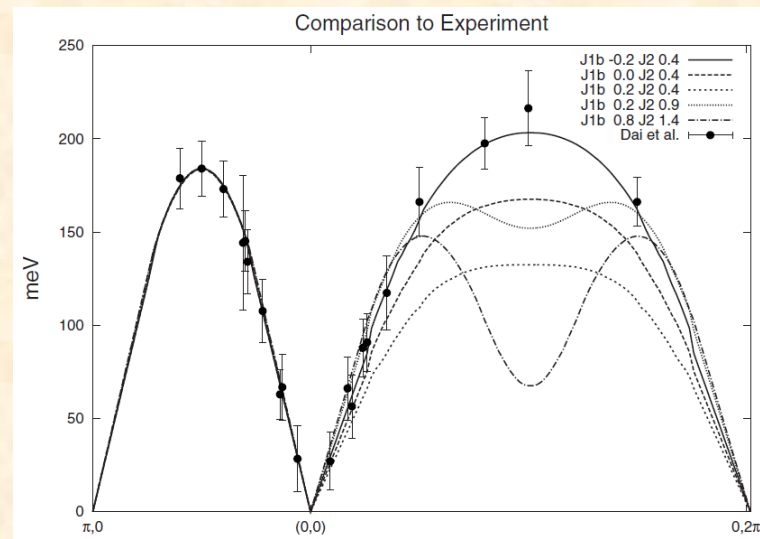
Para.



AFM



dispersion



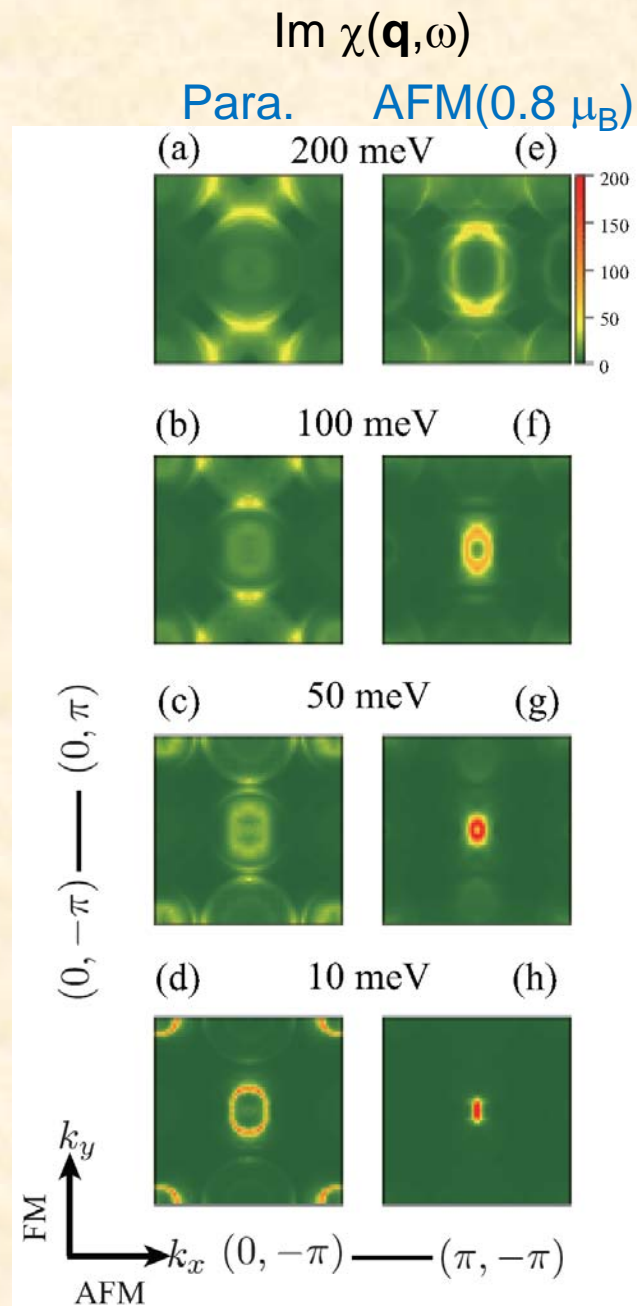
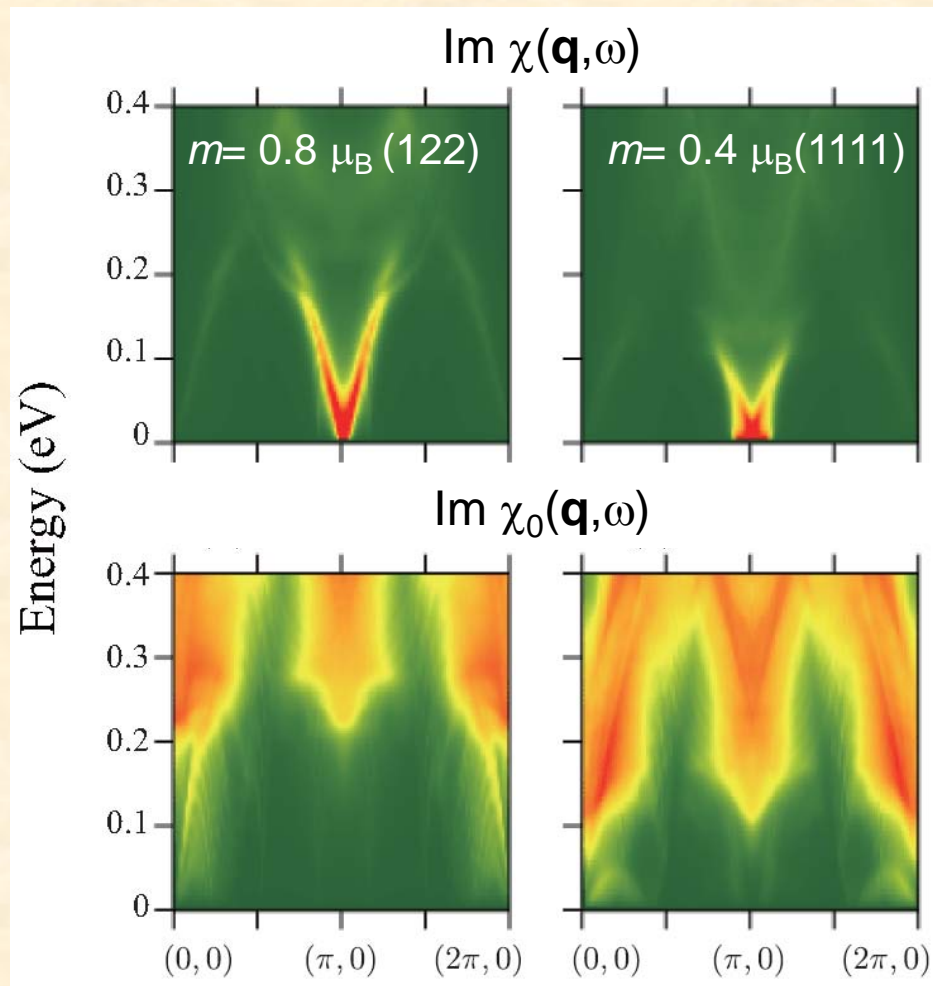
J. Zhao *et al.*, Nat. Phys.
5, 555 (2009)

Localized spin model

Spin excitation for AF metal Theory

E. Kaneshita and T.T., arXiv:1002.2701

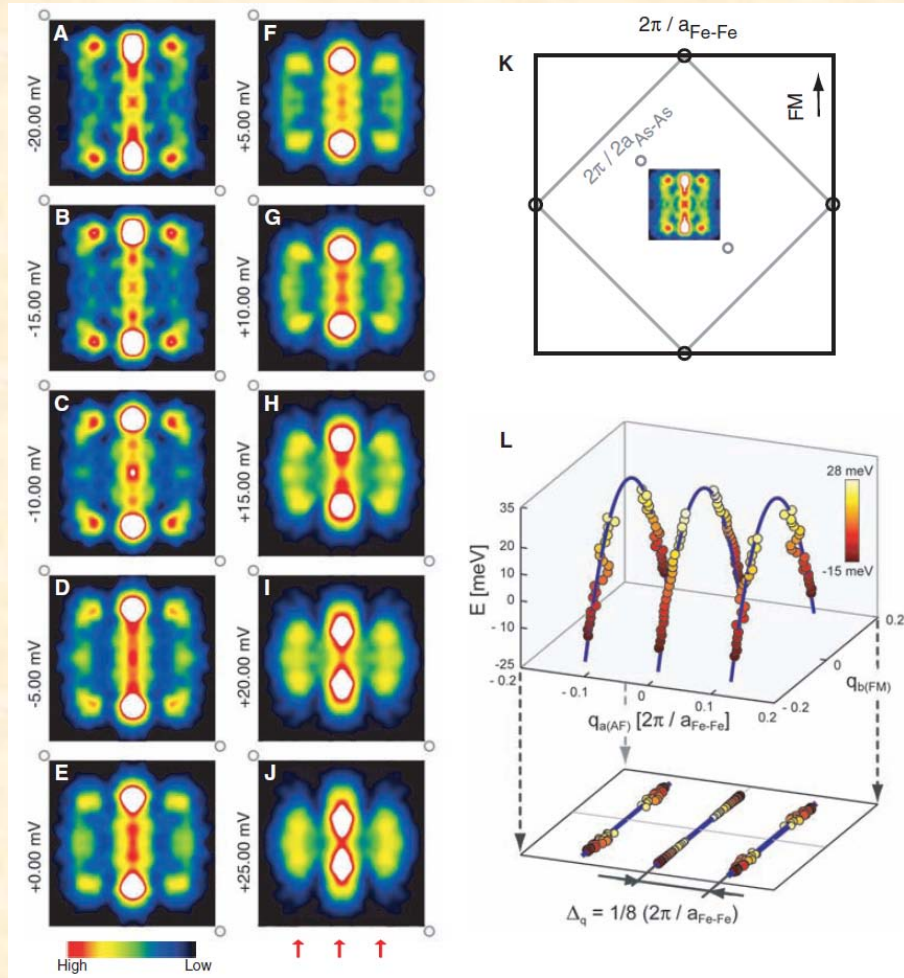
Five band + mean-field $\mathbf{Q}=(\pi,0)$ “Stripe”order
Random phase approximation



“Nematic” electronic nanostructure seen in AF metal

STM for $\text{CaFe}_{1.94}\text{Co}_{0.06}\text{As}_2$

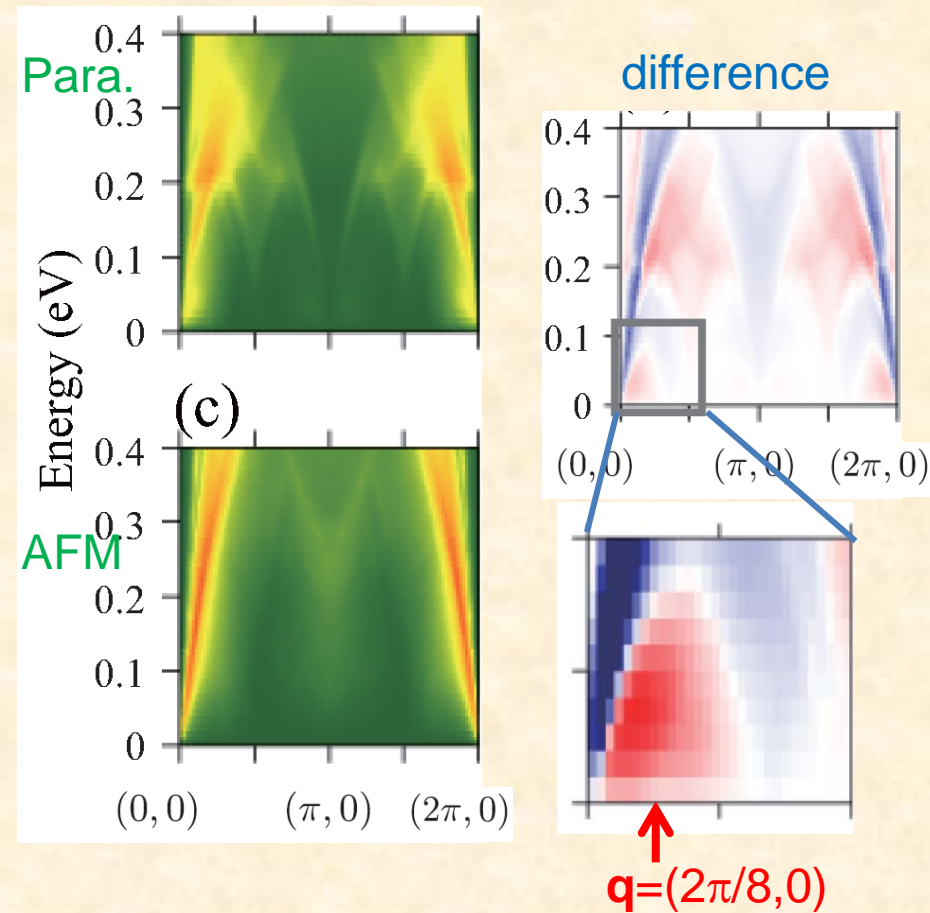
T.-M. Chuang *et al.*, Science 327, 181 (2010)



charge modulation with 8 Fe-Fe distance

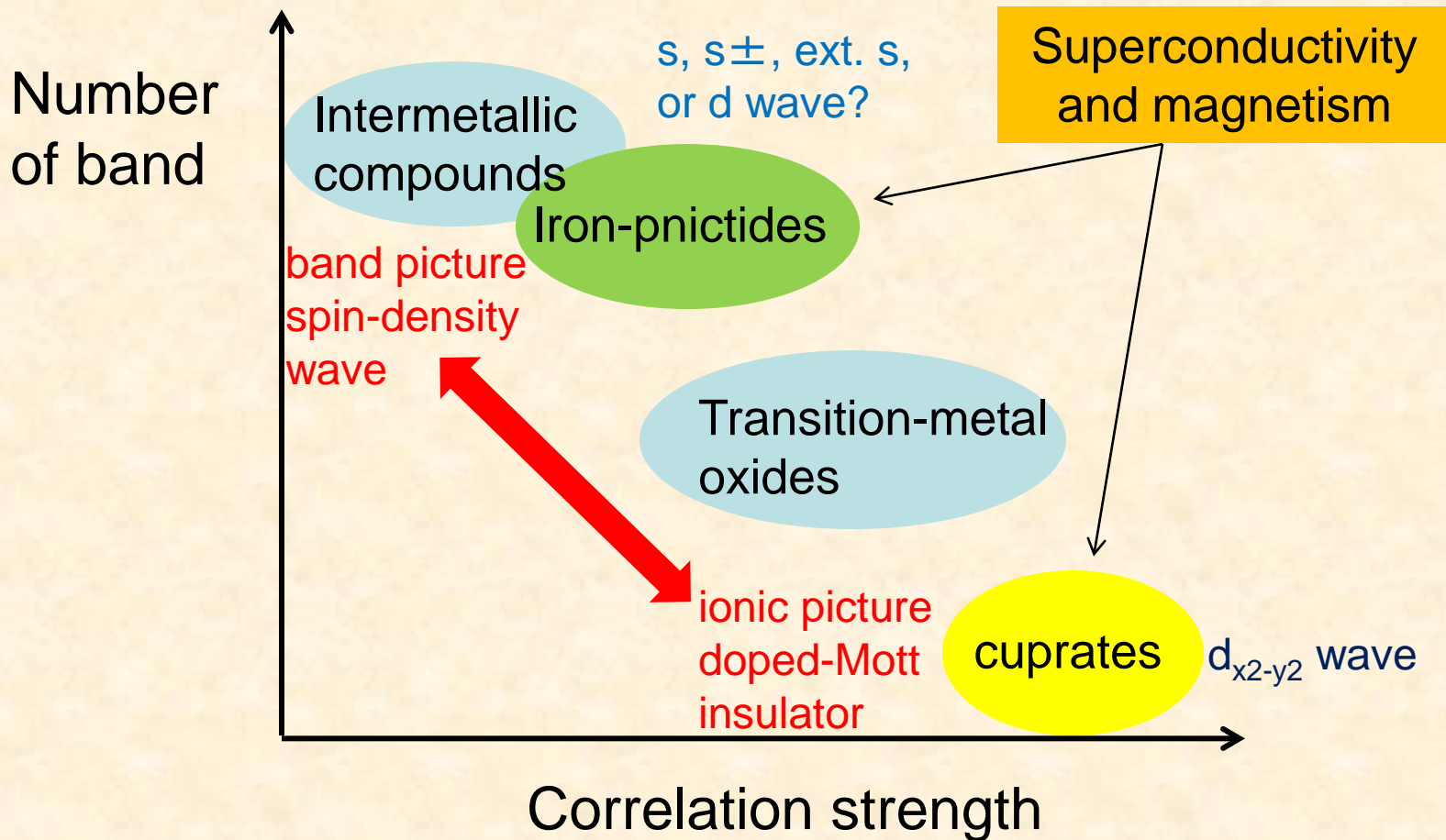
Charge response function

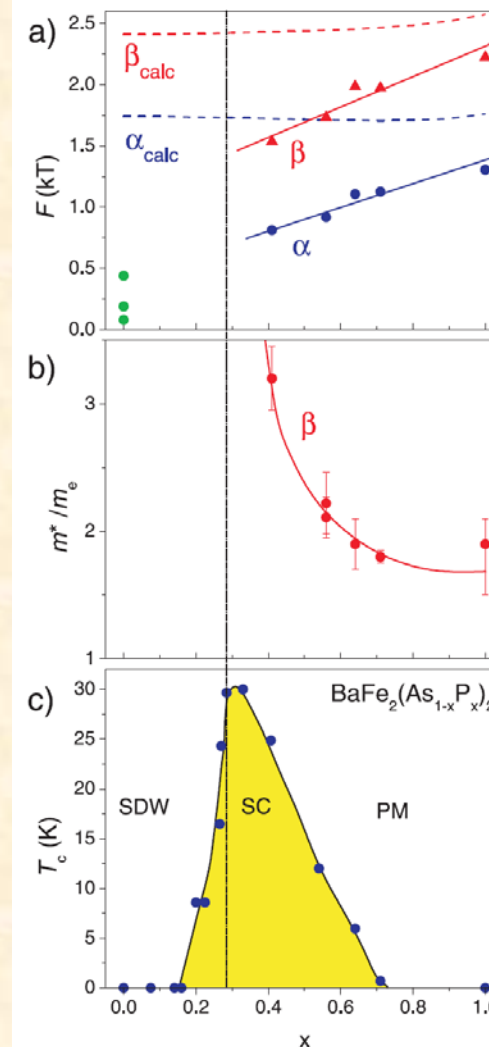
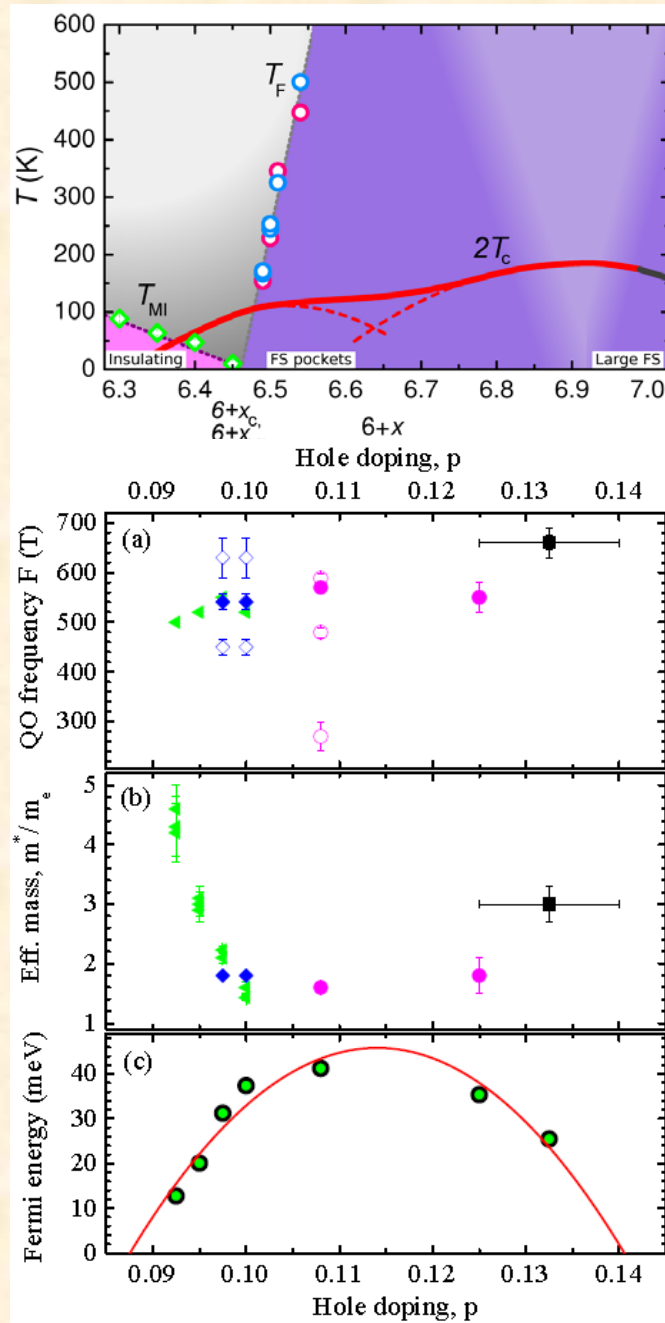
E. Kaneshita and T.T., arXiv:1002.2701



Charge fluctuations from residual Fermi surfaces

Summary





H. Shishido *et al.*,
PRL 104, 057008
(2010)

- Multiple Fermi surfaces
- Divergence of the effective mass

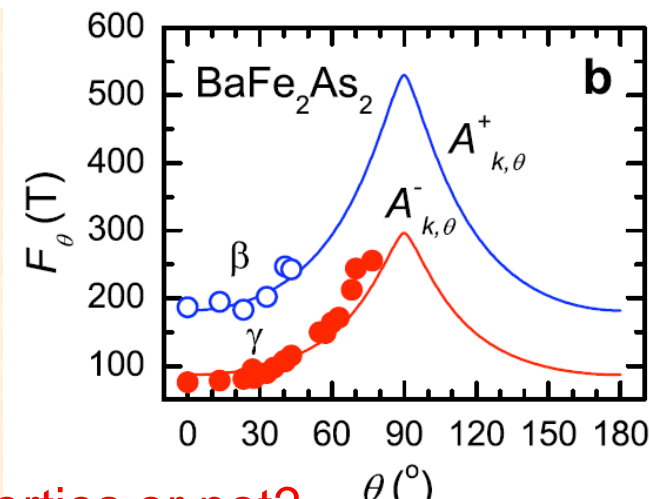
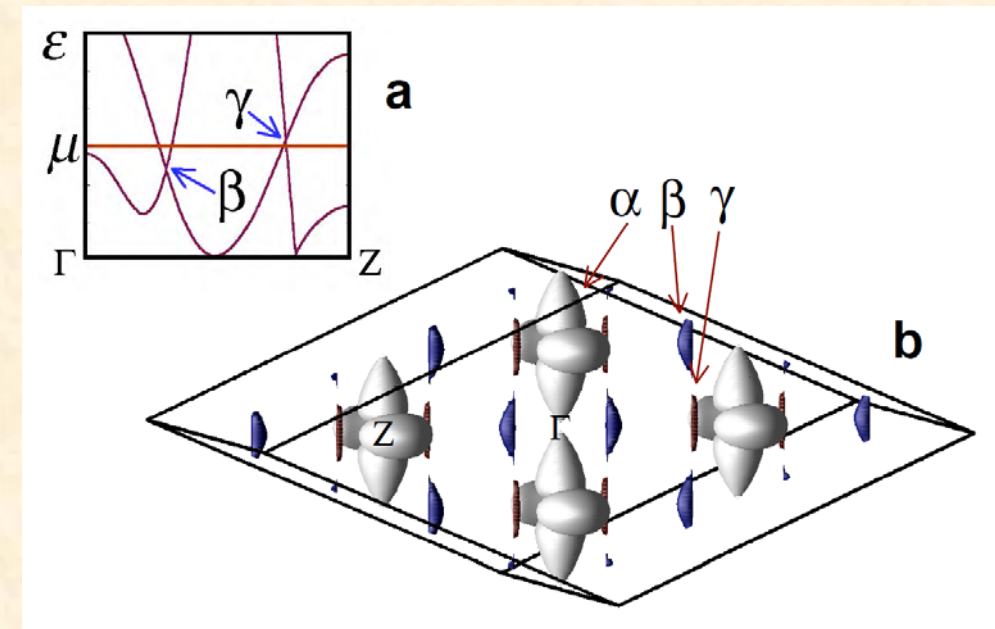
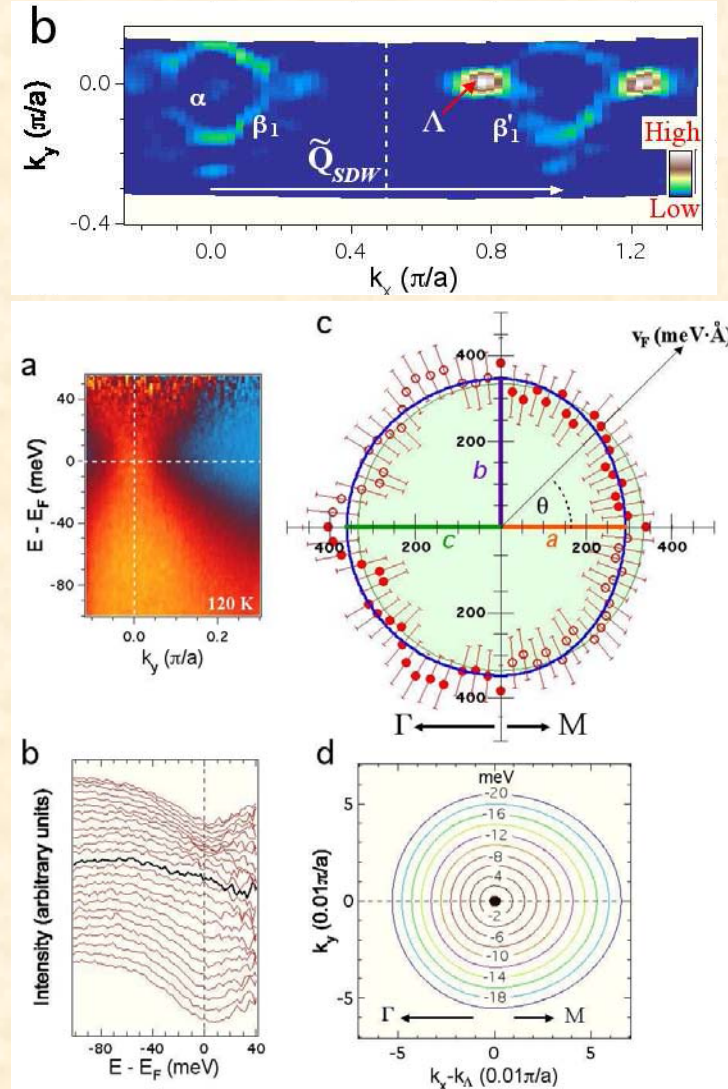
Similar to iron-pnictides?

S. E. Sebastian *et al.*, arXiv:0910.2359
J. Singleton *et al.*, arXiv:0911.2745

Perspective for iron-pnictides

Dirac particles in band dispersions of AFM BaFe_2As_2

P. Richard *et al.*, arXiv:0909.0574



Real effect on transport properties or not?

N. Harrison and S. E. Sebastian,
arXiv:0910.4199